

Orbital ordering in the two-dimensional ferromagnetic semiconductor Rb_2CrCl_4

U. SCHWINGENSCHLÖGL and V. EYERT (*)

Institut für Physik, Universität Augsburg, 86135 Augsburg, Germany

PACS. 71.20.-b – Electron density of states and band structure of crystalline solids.

PACS. 71.20.Be – Transition metals and alloys.

Abstract. – We present the results of electronic structure calculations for the two-dimensional ferromagnet Rb_2CrCl_4 . They are obtained by the augmented spherical wave method as based on density functional theory and the local density approximation. In agreement with experimental data Rb_2CrCl_4 is found to be semiconducting and displays long-range ferromagnetic order of the localized Cr $3d$ moments. The magnetic properties are almost independent of the structural modifications arising from the Jahn-Teller instability, which leads from the parent body-centered tetragonal K_2NiF_4 structure to a side-centered orthorhombic lattice. In contrast, our calculations give evidence for a strong response of the optical band gap to the corresponding structural changes.

Introduction. – Since the discovery of CrBr_3 as a ferromagnetic semiconductor by Tsubokawa [1] this narrow class of materials has attracted increasing interest. To some part this is for fundamental reasons, since these compounds serve as ideal candidates for the Heisenberg model. However, the prospect of using ferromagnetic semiconductors in spin electronics has motivated an even greater amount of research activities in the last years. Only recently, $\text{La}_2\text{MnNiO}_6$ has been shown to exhibit long-range ferromagnetic order below $T_C \approx 280$ K with a magnetization of $5 \mu_B$ per formula unit [2] and an optical band gap of about 0.6 eV as determined by electronic structure calculations [3].

Rubidium tetrachlorochromide, Rb_2CrCl_4 , also belongs to this class of non-metallic ferromagnets albeit with a much lower ordering temperature of $T_C = 52.4$ K [4, 5]. According to neutron scattering measurements of the spin-wave dispersion this compound behaves as a two-dimensional, $S = 2$, easy-plane ferromagnet with an in-plane exchange constant of $J = 7.7$ K [6]. Since the interlayer coupling was estimated to be about four orders of magnitude smaller than the intralayer interaction, three-dimensional long-range order was also attributed to the weak uniaxial anisotropy. The latter, in addition, leads to a small energy gap of about 0.1 meV in the spin wave dispersion at the center of the Brillouin zone, which precludes true XY-type behaviour [5, 7]. Furthermore, the anisotropy causes a canting of the ordered spins of 5.2° away from the $\langle 110 \rangle$ direction [7]. From susceptibility measurements and neutron scattering investigations of the static critical properties a crossover from an ideal

(*) E-mail: Volker.Eyert@physik.uni-augsburg.de

two-dimensional XY-like behaviour to a narrow three-dimensional region on approaching T_C from either side of the transition was inferred [8–10].

The crystal structure of Rb_2CrCl_4 is closely related to the body-centered tetragonal structure of K_2NiF_4 with space group D_{4h}^{17} ($I4/mmm$). In this structure the magnetic ions are arranged on a square planar lattice and coupled via the anions located midway between them. However, the Cr d^4 electronic configuration in Rb_2CrCl_4 with triply occupied t_{2g} states and an orbital degeneracy in the singly occupied e_g states is susceptible to a Jahn-Teller instability. Indeed, the situation is not unlike that found for K_2CuF_4 , which has a Cu d^9 configuration. While for the copper compound early experiments were interpreted in favour of the K_2NiF_4 structure with octahedra compressed parallel to the c -axis, Khomskii and Kugel argued on the basis of theoretical considerations that this structure was incompatible with the observed ferromagnetic order [11, 12]. Subsequently performed neutron and x-ray diffraction studies confirmed these ideas and gave evidence for a side-centered orthorhombic lattice with space group D_{2h}^{18} (Cmca) and two formula units per cell [13, 14]. In this structure, the octahedra are elongated with the long axis lying in the plane and pointing alternatively parallel to the a - and b -axis of the parent K_2NiF_4 unit cell. For Rb_2CrCl_4 , first evidence for the orthorhombic structure came from NMR experiments, which revealed that the local environments of the chromium sites are elongated chlorine octahedra having almost tetragonal symmetry [15]. Later on, the space group D_{2h}^{18} (Cmca) was also confirmed for Rb_2CrCl_4 [7, 16, 17].

In this space group the Rb atoms occupy the Wyckoff positions (8d), $(0, 0, \pm z_{\text{Rb}})$, with $z_{\text{Rb}} = 0.3568$ and the Cr atoms are located at the (4a) sites at $(0, 0, 0)$. The apical Cl atoms are found at the Wyckoff positions (8d) with $z_{\text{Cl}} = 0.1508$, whereas the equatorial Cl atoms occupy the (8f) positions at $(1/4 + \delta, 1/4 + \delta, 0)$. Here, the distortion parameter δ characterizes the deviation from the ideal K_2NiF_4 -structure; the experimental value of $\delta = 0.0154$ corresponds to a 0.16 \AA shift of the Cl ions off the central positions between two neighbouring Cr sites [7]. As a consequence, the in-plane Cr-Cl bond distances amount to 2.70 and 2.39 \AA , whereas the apical distance is 2.37 \AA .

Despite their analogous crystal structures there is one important difference distinguishing Rb_2CrCl_4 from K_2CuF_4 . In the latter compound, the single unpaired electron in the d^9 configuration of the Cu^{2+} ion occupies the $d_{z^2-x^2}$ or $d_{z^2-y^2}$ orbital, depending on the orientation of the local octahedron. Due to the peculiarities of the crystal structure the local axes of neighbouring Cu sites are orthogonal and so are the orbitals. Hence, according to the Goodenough-Kanamori-Anderson (GKA) rules ferromagnetic order results. In contrast, the d^4 configuration of the Cr^{2+} ions is characterized by a single e_g electron in a $d_{3y^2-r^2}$ or $d_{3x^2-r^2}$ orbital. Yet, despite their 90° rotation, orbitals of this kind placed at neighbouring sites are not orthogonal and the GKA rules would be in favour of an antiferromagnetic coupling.

In order to resolve this issue in a more systematic manner, Feldkemper and Weber started from a multiband Hubbard model, which included both the metal d and the ligand p orbitals [18]. Using a Rayleigh-Schrödinger perturbation expansion to map this model onto an effective Heisenberg Hamiltonian they were able to describe the superexchange coupling between magnetic sites. Due to the inclusion of various interaction paths their calculations extended the basic GKA rules and resulted in a net ferromagnetic interplanar coupling in agreement with the experimental findings.

In this Letter, we take account of the obvious lack of first principles studies for Rb_2CrCl_4 and complement the model approaches by electronic structure calculations, thereby continuing previous work on ferromagnetic semiconductors [19–22]. In doing so, we aim especially at extending the current understanding of the interplay between the Jahn-Teller distortion and the optical band gap as well as the magnetic ordering. Previous electronic structure calculations for K_2CuF_4 , which confirmed the non-metallic ferromagnetic ground state, demonstrated,

that neither the lattice distortion due to the Jahn-Teller instability nor the magnetic order alone are sufficient to produce the optical band gap [20]. Since ferromagnetic ordering was also found for the ideal K_2NiF_4 structure ($\delta = 0$), it is the semiconducting ground state, which requires the Jahn-Teller effect, and not the magnetic order. Our results for Rb_2CrCl_4 are in line with this interpretation.

Methodology. – The calculations are based on density functional theory and the local density approximation as implemented in the scalar-relativistic augmented spherical wave method [23, 24]. In order to represent the correct shape of the crystal potential in the large voids of the open crystal structure, additional augmentation spheres were inserted. Optimal augmentation sphere positions as well as radii of all spheres were automatically generated by the sphere geometry optimization (SGO) algorithm [25]. Self-consistency was achieved by an efficient algorithm for convergence acceleration [26]. Brillouin zone sampling was done using an increasing number of \mathbf{k} -points ranging up to 576 points within the irreducible wedge.

Results and Discussion. – Partial densities of states as grown out of both spin-degenerate and spin-polarized calculations are displayed in Fig. 1. Of the three groups of bands the first

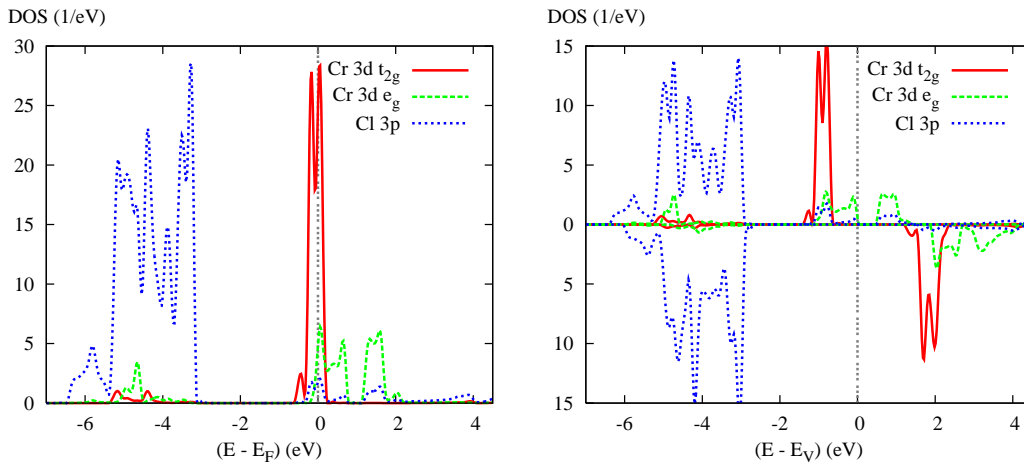


Fig. 1 – Partial Cr $3d$ and Cl $3p$ DOS for the experimental crystal structure ($\delta = 0.0154$). Here and in the following figures results of spin-degenerate and spin-polarized calculations are given on the left and right, respectively.

one extending from about -6.5 eV to -3 eV originates predominantly from the Cl $3p$ states. In contrast, the second and third group as found at and above the Fermi level trace back mainly to the Cr $3d t_{2g}$ and e_g states. d - p hybridization, leading to admixtures of these states in the energy region, where the respective other partner dominates, is much reduced. Finally, taking into account spin-polarization by allowing for long-range ferromagnetic order, we observe an almost rigid exchange splitting of the d states of ≈ 2.8 eV going along with a total energy lowering of about 0.3 Ryd per unit cell. The calculated magnetic moment of $3.718\mu_B$ per chromium site agrees perfectly well with the value of $3.7 \pm 0.4\mu_B$ as deduced from neutron diffraction data [27].

Concentrating on the small energy region of the Cr $3d$ states we display in Figs. 2 and 3 the electronic band structure and the partial Cr $3d$ densities of states. For the former we use the Brillouin zone of the side-centered orthorhombic lattice with the high-symmetry points $Z = (1/2, 0, 1/2)$, $X = (1/2, 0, 0)$, $P = (1/2, 1/2, 0)$, and $N = (0, 1/2, 0)$ (see Figs. 4

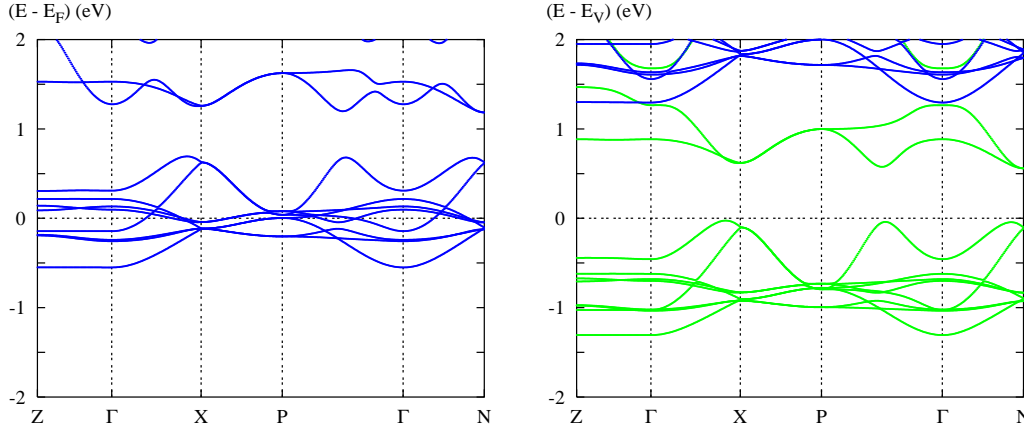


Fig. 2 – Electronic structure for the experimental crystal structure ($\delta = 0.0154$). In the spin-polarized calculation spin-majority and spin-minority bands are given in green and blue, respectively.

and 5 of Ref. [20] for more details on the relation between the Brillouin zones of K_2NiF_4 and $\text{K}_2\text{CuF}_4/\text{Rb}_2\text{CrCl}_4$). The almost vanishing dispersion along the line Γ - Z reflects the two-dimensional nature of the crystal structure. In the representation of the partial densities of states we use the local coordinate system with the z axis pointing parallel to the elongated distance of the local CrCl_6 octahedron. We distinguish the narrow Cr $3d$ t_{2g} states from the $d_{3z^2-r^2}$ and $d_{x^2-y^2}$ contributions. Due to the elongation of the octahedra the $d_{3z^2-r^2}$ states are shifted to lower energies as compared to the $d_{x^2-y^2}$ states. As a consequence, we observe energetical overlap of the $d_{3z^2-r^2}$ states with the t_{2g} bands and a gap of about 0.5 eV between the e_g states.

While the spin-degenerate calculations lead to metallic behaviour, the exchange splitting places the Fermi energy between the spin-majority $d_{3z^2-r^2}$ and $d_{x^2-y^2}$ states, leaving an optical band gap of 0.56 eV. Our results thus clearly confirm the orbital ordering as deduced

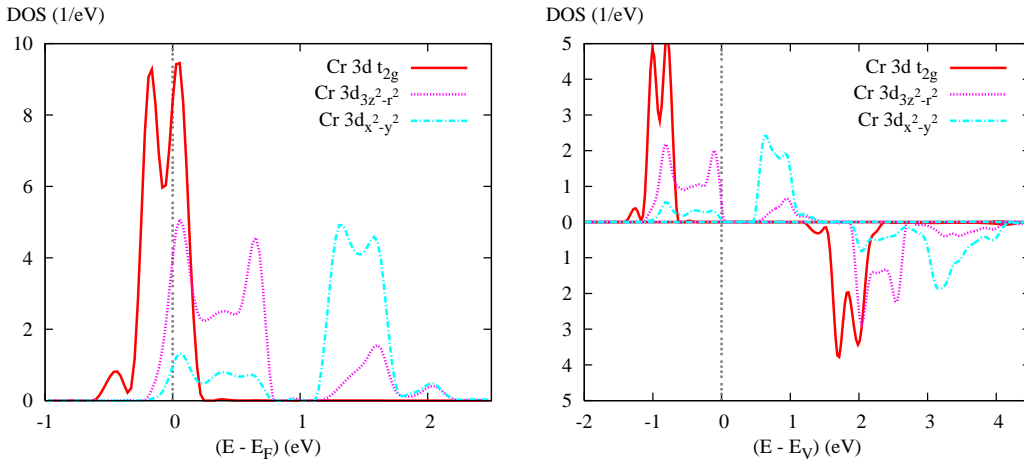


Fig. 3 – Partial Cr $3d$ DOS for the experimental crystal structure ($\delta = 0.0154$). The t_{2g} contribution is scaled to one orbital.

from the polarized neutron diffraction data by Münnighoff *et al.* with all five d orbitals singly occupied except for the $d_{x^2-y^2}$ orbital, which is empty [28].

In addition to the above calculations we have considered an antiferromagnetic order with antiparallel spin alignment of the two Cr sites inside the side-centered orthorhombic unit cell. Again, the bands experience an almost rigid spin splitting, which gives room for an optical gap of 0.43 eV. The magnetic moments per chromium site amount to $\pm 3.627\mu_B$. Yet, the energy of the antiferromagnetic solution is by 27 meV higher than that found for the ferromagnetic situation.

All calculations presented so far were based on the experimental crystal structure, i.e. for $\delta = 0.0154$. In order to study the effect of the distortion on the electronic and magnetic properties we performed additional calculations for several values of δ varying from zero to 1.5 times the experimental value. The results are summarized in Table I, which comprises spin-polarized

Distortion δ	$E_{\text{fe}} - E_{\text{nm}}$	$\mu_{\text{Cr,fe}}$	Δ_{fe}	$E_{\text{af}} - E_{\text{nm}}$	$\mu_{\text{Cr,af}}$	Δ_{af}
0.0000	-0.301	3.736	-	-0.263	3.602	0.015
0.0038	-0.304	3.717	0.202	-0.269	3.604	0.127
0.0077	-0.304	3.718	0.246	-0.269	3.609	0.150
0.0115	-0.305	3.717	0.280	-0.271	3.610	0.179
0.0154	-0.310	3.718	0.558	-0.283	3.627	0.427
0.0192	-0.308	3.722	0.363	-0.278	3.621	0.265
0.0231	-0.308	3.723	0.374	-0.214	3.625	0.273

TABLE I – Total energies (in Ryd per 2 Cr), magnetic moments (in μ_B), and optical band gap (in eV) for different distortion parameters δ . The experimental crystal structure corresponds to $\delta = 0.0154$.

calculations with both ferro- and antiferromagnetic order. Obviously, the total energies for both situations assume a minimum for the experimental value of δ . However, for the antiferromagnetic solutions total energies are by ≈ 27 meV above those for the ferromagnetic case. In contrast, the optical band gap for both kinds of spin-polarized calculations assumes a maximum value at $\delta = 0.0154$; it vanishes for ferromagnetic order in the ideal K_2NiF_4 structure as has been also observed in our previous work on K_2CuF_4 [20]. Surprisingly, the magnetic moments at the Cr sites are almost independent of the distortion parameter δ , i.e. of the Cr-Cl bond lengths. This is due to the localized nature of these moments, which forms the basis for the treatment within the Heisenberg model, and reflects the finding of Feldkemper and Weber that a reasonable variation of hopping parameters changes the magnetic coupling only slightly [18].

Finally, we aim at understanding the role of the Jahn-Teller effect for the changes of the electronic states. To this end, we display band structures calculated for hypothetical crystal structures with zero distortion parameter δ in Fig. 4. On comparing these results to Fig. 2 we recognize as the main effect of the Jahn-Teller distortion the splitting of the bands in the middle of the line P- Γ as well as near the X- and N-points. While in the spin-degenerate case this splitting occurs at about 1 eV above the Fermi energy, it opens the optical band gap for the ferromagnetically ordered state. Surprisingly, the spin-majority bands for $\delta = 0$ and finite distortion as displayed in these figures look very similar to the spin-degenerate bands of K_2NiF_4 , where the band degeneracies occur exactly at the X- and N-points and thus give rise to perfect Fermi-surface nesting [20]. While the nesting is not complete here, one would nevertheless be tempted to interpret the Jahn-Teller effect as resulting from a Fermi-surface instability of the spin-majority bands. However, we point out that, due to the comparatively low Curie temperature of Rb_2CrCl_4 , we cannot use the spin-polarized calculation as a starting point but would rather need the band structure of a paramagnetic system, which is not

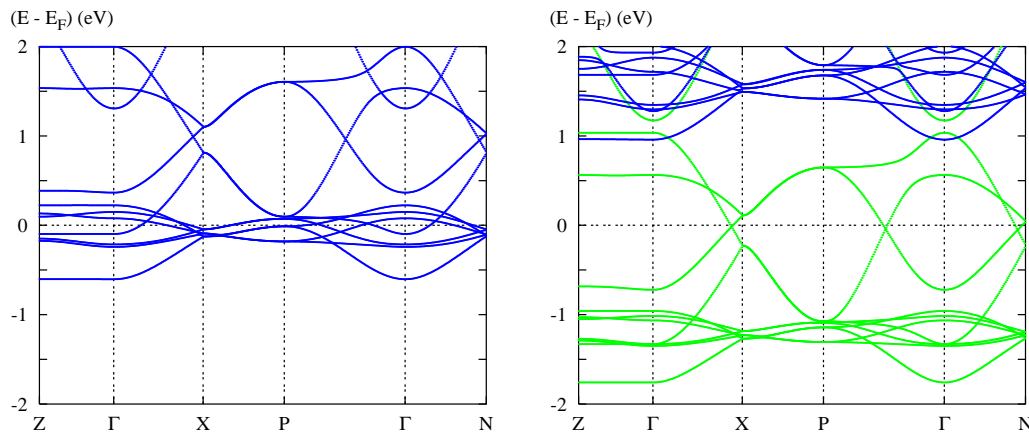


Fig. 4 – Electronic band structure for the idealized tetragonal crystal structure (distortion $\delta = 0$).

available.

Conclusion. – In conclusion, we have reported on the first density functional based electronic structure calculation for the ferromagnetic semiconductor Rb_2CrCl_4 . In agreement with the available experimental data we obtain a two-dimensional dispersion of the electronic bands and a non-metallic ferromagnetically ordered ground state. The well localized magnetic moments of $\approx 3.7\mu_B$ are carried by the Cr $3d$ t_{2g} and $d_{3z^2-r^2}$ orbitals, in perfect agreement with the magnetic moments and orbital occupations deduced from neutron diffraction experiments. Studying the influence of the Jahn-Teller distortion we find only minor influence on the size and ferromagnetic order of the magnetic moments, thus confirming the model approach by Feldkemper and Weber. In contrast, the electronic band structure experiences drastic changes on switching on the Jahn-Teller distortion turning, in particular, from metallic to semiconducting.

Fruitful discussions with W. Weber are gratefully acknowledged. This work was supported by the Deutsche Forschungsgemeinschaft through SFB 484.

REFERENCES

- [1] TSUBOKAWA I., *J. Phys. Soc. Jap.*, **15** (1960) 1664
- [2] ROGADO N. S., LI, J., SLEIGHT A. W., and SUBRAMANIAN, M. A., *Adv. Mater.*, **17** (2005) 2225
- [3] MATAR S. F., SUBRAMANIAN, M. A., EYERT V., WHANGBO M., and VILLESUZANNE A., *cond-mat/0509431*,
- [4] GREGSON, A. K., DAY P., LEECH D. H., FAIR M.J., and GARDNER W. E., *J. Chem. Soc. (Dalton)*, (1975) 1306
- [5] HUTCHINGS M. T., ALS-NIELSEN J., LINDGARD P. A., and WALKER P. J., *J. Phys. C: Solid State Phys.*, **14** (1981) 5327
- [6] HUTCHINGS M. T., FAIR M. J., DAY P., and WALKER P. J., *J. Phys. C: Solid State Phys.*, **9** (1976) L55

- [7] JANKE E., HUTCHINGS M. T., DAY P., and WALKER P. J., *J. Phys. C: Solid State Phys.*, **16** (1983) 5959
- [8] KLEEMANN W., OTTE D., USADEL K. D., and BRIESKORN G., *J. Phys. C: Solid State Phys.*, **19** (1986) 395
- [9] ALS-NIELSEN J., BRAMWELL S. T., HUTCHINGS M. T., MCINTYRE G. J., and VISSER D., *J. Phys.: Condens. Matt.*, **5** (1993) 7871
- [10] BRAMWELL S. T., HOLDSWORTH P. C. W., and HUTCHINGS M. T., *J. Phys. Soc. Japan*, **64** (1995) 3066
- [11] KHOMSKII D. I. and KUGEL K. I., *Solid State Commun.*, **13** (1973) 763
- [12] KUGEL K. I. and KHOMSKII D. I., *Sov. Phys. Usp.*, **25** (1982) 231
- [13] ITO Y., and AKIMITSU J., *J. Phys. Soc. Japan*, **40** (1976) 1333
- [14] HIDAKA M., and WALKER P. J., *Solid State Commun.*, **31** (1979) 383
- [15] LE DANG K., VEILLET P., and WALKER P. J., *J. Phys. C: Solid State Phys.*, **10** (1977) 4593
- [16] DAY P., HUTCHINGS M. T., JANKE E., and WALKER P. J., *J. Chem. Soc. Chem. Commun.*, (1979) 711
- [17] MÜNNINGHOFF G., TREUTMANN W., HELLNER E., HEGER G., and REINEN D., *J. Solid State Chem.*, **34** (1980) 289
- [18] FELDKEMPER S. and WEBER W., *Phys. Rev. B*, **57** (1998) 7755
- [19] KÜBLER J., EYERT V. and STICHT J., *Physica C*, **153-155** (1988) 1237
- [20] EYERT V. and HÖCK K.-H., *J. Phys.: Condens. Matt.*, **5** (1993) 2987
- [21] EYERT V., HÖCK K.-H., and RISEBOROUGH P. S., *Europhys. Lett.*, **31** (1995) 385
- [22] EYERT V., SIBERCHICOT B., and VERDAGUER M., *Phys. Rev. B*, **56** (1997) 8959
- [23] WILLIAMS A. R., KÜBLER J., and GELATT C. D. JR., *Phys. Rev. B*, **19** (1979) 6094
- [24] EYERT V., *Int. J. Quant. Chem.*, **77** (2000) 1007
- [25] EYERT V. and HÖCK K.-H., *Phys. Rev. B*, **57** (1998) 12727
- [26] EYERT V., *J. Comp. Phys.*, **124** (1996) 271
- [27] FAIR M. J., GREGSON A. K., DAY P., and HUTCHINGS M. T., *Physica B*, **86-88** (1977) 657
- [28] MÜNNINGHOFF G., HELLNER E., FYNE P. J., DAY P., HUTCHINGS M. T., and TASSET F., *J. Phys. (France) Coll. C*, **7** (1982) 243